ACS SENSORS

Article

pubs.acs.org/acssensors

Solid State Sensor for Simultaneous Measurement of Total Alkalinity and pH of Seawater

Ellen M. Briggs,[†] Sergio Sandoval,[‡] Ahmet Erten,[§,#] Yuichiro Takeshita,[†,¶] Andrew C. Kummel,[∥] and Todd R. Martz*[,†]

[†]Scripps Institution of Oceanography, [‡]California Institute for Telecommunications and Information Technology (Cal IT2), [§]Electrical and Computer Engineering Department, and [∥]Materials Science and Engineering, University of California San Diego, La Jolla, California 92093-0244, United States

ABSTRACT: A novel design is demonstrated for a solid state, reagent-less sensor capable of rapid and simultaneous measurement of pH and Total Alkalinity (A_T) using ion sensitive field effect transistor (ISFET) technology to provide a simplified means of characterization of the aqueous carbon dioxide system through measurement of two "master variables": pH and A_T. ISFET-based pH sensors that achieve 0.001 precision are widely used in various oceanographic applications. A modified ISFET is demonstrated to perform a nanoliter-scale acid−base titration of A_T in under 40 s. This method of measuring A_T, a Coulometric Diffusion Titration, involves electrolytic generation of titrant, H^+, through the electrolysis of water on the surface of the chip via a microfabricated electrode eliminating the requirement of external reagents. Characterization has been performed in seawater as well as titrating individual components (i.e., OH^-, HCO_3^-, CO_3^{2-}, $B(OH)_4^-$, PO_4^{3-}) of seawater A_T. The seawater measurements are consistent with the design in reaching the benchmark goal of 0.5% precision in A_T over the range of seawater A_T of ∼2200−2500 μmol kg^{-1} which demonstrates great potential for autonomous sensing.

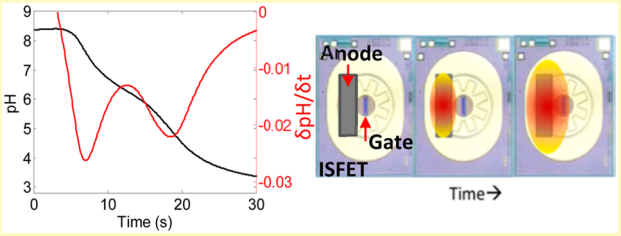

KEYWORDS: *ISFET, total alkalinity, pH, seawater, sensor*

Ship-based platforms have traditionally been used for open-ocean monitoring of the carbon cycle resulting in large gaps of observations in space and time. Discrete sampling is often insufficient for resolving many important features of marine biogeochemical cycles and subsequent feedback that occur at much shorter time scales.[1,2] Direct, in situ measurements of ocean inorganic carbon chemistry including pH, total dissolved inorganic carbon (C_T), partial pressure of CO_2 (pCO_2), and total alkalinity (A_T) are desirable, but current chemical sensor technology does not fulfill the low power, robust design, accuracy, and stability requirements for use on autonomous platforms.[3−5] Combinations of either pH or pCO_2 with A_T or C_T are preferred for constraining carbonate speciation based on propagation of error of the best available analytical techniques.[6,7] However, A_T and C_T analytical techniques are the most difficult to measure in situ, and no carbon variable can be calculated more accurately than the combined parameters can be measured.[7] Commercially available autonomous sensors for pH and pCO_2 are not capable of simultaneous measurements, and these variables are the least desirable carbon pair for differentiating some key biogeochemical processes such as production and calcification.[6] Therefore, there is a great need to develop new methods compatible with in situ technologies for measuring A_T and C_T autonomously with accuracy and precision comparable to the best analytical methods.

Globally, seawater A_T spans a relatively narrow range ∼2200−2500.[8] In the open surface ocean, A_T is dominantly controlled by simple physical processes (e.g., precipitation, evaporation) and can often be estimated accurately from measurements of temperature and salinity.[9−11] However, such empirical relationships for A_T are not as well-developed beneath the surface and become invalid in many dynamic environments at depth and at the ocean surface where processes such as freshwater input and calcium carbonate formation lead to nonconservative behavior in A_T.[10,12,13] Coccolithophore blooms, sediment porewaters, coral reefs, river mouths, and coastal shelves are general examples where nonconservative behavior is known; however, these regions play a significant role in biogeochemical processes and conservative relationships cannot be applied.

The standard procedure for measuring seawater A_T uses a potentiometric titration monitored by a glass electrode.[14] A_T is calculated from titrant volume and electromotive force (emf) data using either modified Gran functions or a nonlinear least-squares approach. Other approaches have been developed using chronopotentiometry[15] as well as spectrophotometry for single-point[16] and tracer monitored titrations;[17,18] however, many of these techniques are limited to benchtop measurements due to instrument complexity, inability to miniaturize, power consumption, and excess reagents. Furthermore, few alternative

Received: May 7, 2017
Accepted: August 14, 2017
Published: August 14, 2017

DOI: 10.1021/acssensors.7b00305
ACS Sens. 2017, 2, 1302−1309

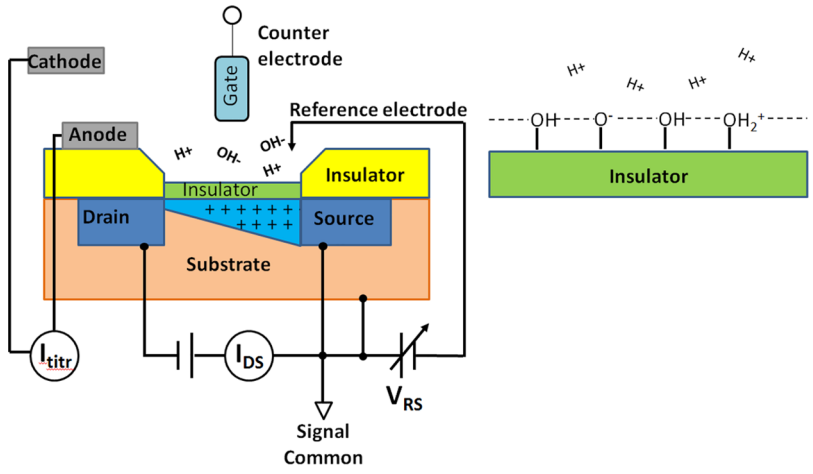

Figure 1. Schematic of operating principle of ISFET. Protons in solution control the degree of protonation and charge distribution at the insulator-solution interface. The resultant potential controls the flow of current between the source and drain of the ISFET and the pH is proportional to the source to reference potential, V_{RS}. A coulometric actuator device comprising an anode−cathode pair and constant current source, I_{titr}, can be integrated with an ISFET to perform a titration on the chip.

techniques capable of autonomous measurements have reached the certainty and level of long-term accuracy and precision of the standard benchtop titration. The chronopotentiometric method, utilizing ion sensitive membranes,[19,20] and tracer monitored titration approach[17,18] show promise for autonomous application and have recently been demonstrated to work in natural waters.

Ion sensitive field effect transistor (ISFET) technology is becoming increasingly popular in pH sensing devices.[21] For instance, Honeywell has commercialized the DuraFET which is a pH sensing ISFET-based combination electrode currently used in industrial as well as oceanographic applications.[22−25] As solid state pH sensors, ISFETs offer advantages relative to glass electrodes including reduced drift as well as the ruggedness required for in situ, autonomous use. Notably, glass electrodes suffer from notoriously high impedance (up to giga ohms) whereas ISFET-based pH sensors are inherently low impedance (tens to hundreds of ohms) leading to significantly improved stability over time.

An ISFET is analogous to the better known metal oxide semiconductor field effect transistor (MOSFET) with the metal oxide gate replaced by a conventional reference electrode. As described by Johnson et al.,[25] the Honeywell Durafet ISFET consists of an N doped silicon substrate which includes two P doped regions which are referred to as the source and drain as shown in Figure 1. Between these two regions is a conduction region referred to as the channel. On top of this channel is an insulator (from here on referred to as the gate) which might be a deposited metal oxide or a nonoxide insulator such as silicon nitride.[21] This channel insulator will exchange hydrogen ion and develop a potential at the insulator solution interface. The resultant interfacial potential controls the shape of the conductance channel of the FET and thus the flow of current between the source and drain. Outside this channel region is a deposited field insulator (identified in Figure 1 as "Insulator"). This field insulator may or may not employ the same material as the channel insulator.

Here ISFET technology is modified to design and test a solid state, reagentless sensor capable of rapid and simultaneous measurement of A_T and pH. By integrating a coulometric actuator device with an ISFET (I_{titr} in Figure 1), a nanoliter-scale acid−base titration can be simultaneously executed and measured on a single ISFET chip. Microfabrication enables the actuator to be placed within microns of the gate thereby reducing the sample volume to nanoliters and decreasing the response time to 40 s. The sensor is optimized for and evaluated over a narrow range of A_T, ∼2200−2500 μmol kg^{-1}, representative of open ocean seawater. This dual pH−A_T sensor provides a means of continuous, direct measurement of aqueous carbon dioxide chemistry.

METHODS

Theory. A MOSFET employs a metal oxide channel insulator on top of which a metal is deposited. This metal is referred to as the gate. ISFETs remove this gate electrode and expose the underlying channel insulator to the sample solution.[26,27] This now removed gate, or substitute metal conductor, remains in solution and is referred to as the counter electrode. This counter electrode can be thought of a wetted gate electrode. The function of this counter is the same as the analogous counter electrode employed in analytical voltammetry or amperometry. The counter is a low impedance electrode, which is used for ISFET control. It controls drain voltage and drain current and its EMF is neither defined nor important for proper function of the ISFET. Because the counter electrode EMF is a suitable metal such as the removed gate electrode, it is of low impedance, and allows a pathway for parasitic leakage currents.

In typical ISFET operation, a constant drain to source voltage (V_{DS}) is applied, and a feedback circuit is used to maintain a constant drain to source current (I_{DS}) (see Figure 1). The resultant source to reference electrode voltage (V_{RS}) is proportional to pH as described by the Nernst eq (eq 1) where R is the universal gas constant (8.3146 J K^{-1} mol^{-1}), T is temperature in Kelvin, F is the Faraday constant (96,485 Coulomb mol^{-1}), and a_H and a_{Cl} are the activities of hydrogen and chloride ions.[21,28]

$$V_{RS} \propto \frac{RT\ln(10)}{F}\log(a_H a_{Cl}) \quad (1)$$

By integrating a coulometric actuator device with an ISFET, a nanoliter-scale acid−base titration can be simultaneously executed and measured on a single ISFET chip.[29−32] Titrant, H^+, is generated through the electrolysis of water by applying an anodic current pulse (I_A) to an actuator electrode with respect to a counter electrode in an analyte solution:

$$\text{Anode: } 2H_2O \rightarrow 4H^+ + 4e^- + O_2$$

$$\text{Cathode: } 2H_2O + 2e^- \rightarrow 2OH^- + H_2$$

DOI: 10.1021/acssensors.7b00305
ACS Sens. 2017, 2, 1302−1309

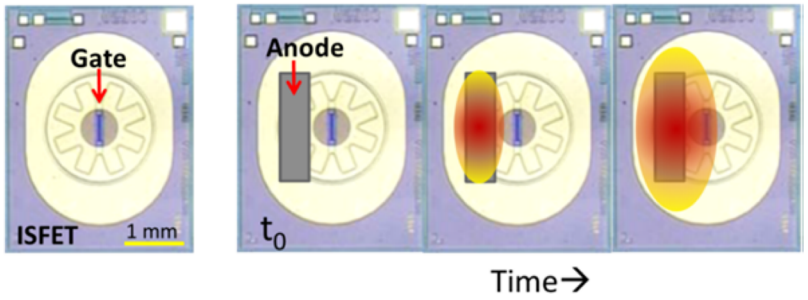

Figure 2. Nonmodified ISFET (left) and conceptual schematic of diffusion of the "titrated zone" (orange) across the gate upon generation of titrant.

By placing the actuator electrode on the surface of the ISFET near the gate, the pH can be rapidly measured as the analyte solution is titrated with the electrolytically generated H^+ as shown in Figure 2.

This "coulometric sensor-actuator system", as it was originally referred to by its inventors,[29,32,33] was later named a "Flash Titration" when commercialized by Orion in the early 2000s.[34] Later, Bakker's group adopted the term Flash Titration to refer to a different method utilizing ion selective membrane chronopotentiometry.[35] Unfortunately, the commercialized product was not successful, due in part to short lifetime and lack of universality demanded by industry.[36] Following significant advances made by Honeywell in ISFET technology and encapsulation methods, field testing by the oceanographic community, coupled with the narrow range of seawater A_T, it is expected that the coulometric sensor-actuator system method can be successfully integrated with the Honeywell ISFET to produce a dual pH–A_T sensor fine-tuned for seawater with increased longevity over its predecessor. Because the Orion Flash Titration system is no longer a product and in order to avoid confusion with the field of ion selective membrane chronopotentiometry, we have chosen to refer to the technique used in the ISFET-based coulometric sensor-actuator system as a coulometric diffusion titration (CDT).

CDT can be described by a one-dimensional diffusive mass transport model.[33] Referring to Figure 3, the topside of the ISFET is viewed on the x-plane and the actuator electrode can be thought of as a semi-infinite plane positioned at $x = 0$ μm parallel to the gate at $x = x_g$ μm. At time t_0, the concentration of a basic analyte is defined as $C_{B,bulk}$ at both the actuator electrode and ISFET gate. At t_{start}, an anodic current pulse is applied to the actuator electrode to generate H^+. At t_1 (blue curve), the proton acceptors are depleted at the anode such that $C_B = 0$ at $x = 0$. This condition is expressed by the Sand equation, t_{Sand}

$$t_{Sand} = \left[\frac{C_{B,Bulk}F\sqrt{\pi D_B}}{2j_c}\right]^2 \quad (2)$$

where D_B is the diffusion coefficient of species B, F is the Faraday constant, and j_c is the current density at the actuator electrode. The reaction horizon moves across the x-plane t_2 (red curve) to t_3 (green curve). The equivalence point is reached at t_{end} when $C_B(x_g, t_3) = 0$ which is the sum of t_{Sand} and t_{delay}, the time it takes for the reaction plane to reach the ISFET gate. Thus, C_B (or A_T) is linearly proportional to $(t_{end})^{1/2}$. A CDT can be completed within 1–60 s depending on the bulk concentration, operating current, and distance between the actuator electrode and gate, x_g. The ISFET response time is on the order of milliseconds and is sufficient to detect the end point of the titration with high accuracy.

Sensor Design. The ISFET die, acquired from Honeywell, was modified by adding an electrode to the topside of the chip proximal to the gate using backend processing techniques. The ISFET chips were assembled into a mechanical mask device as shown in Figure 4 and precisely positioned to expose an area 100–150 μm from the gate of the chip.

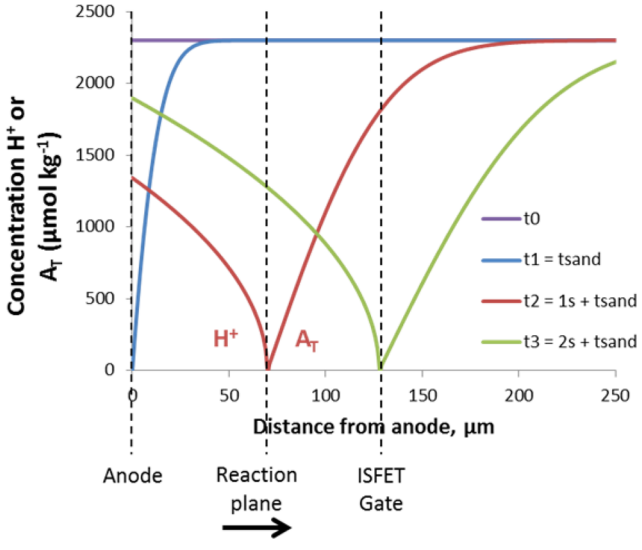

Figure 3. CDT model for seawater showing the time evolution of the concentration profiles of excess titrant (H^+) and analyte (A_T) and their position relative to the anode and ISFET gate. The end point is reached when the zero-point of the concentration profile reaches the ISFET gate (green curve).

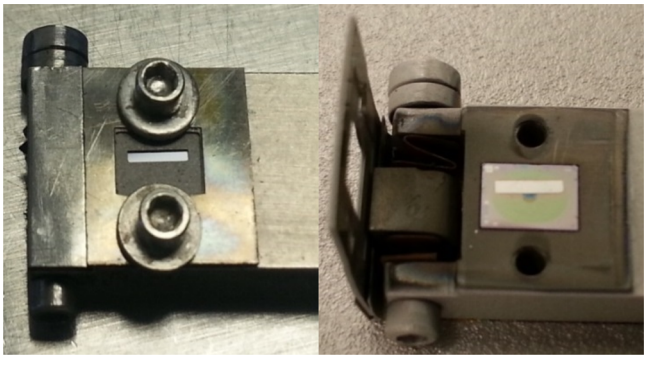

Figure 4. Mechanical mask used to pattern an actuator electrode on the surface of the ISFET. The ISFET was placed in the holder and the electrode was then deposited onto the exposed region of the ISFET precisely aligned within 100–150 μm of the gate.

The exposed ISFET surface was cleaned using an O_2 plasma followed by deposition of a 2.5 μm electrically insulating layer of SiO_2 by plasma enhanced chemical vapor deposition (PECVD) at 350 °C. 50 nm of Ti was deposited and exposed to atmosphere to form an insulating layer of TiO_2. 200 nm of Ti was deposited as an adhesion layer followed by deposition of 500 nm of Pt by argon sputtering. The modified ISFETs were removed from the mechanical mask and then annealed at 350 °C for 3 min. The multistep insulator deposition was performed with a single shadow mask so that all the materials are self-

DOI: 10.1021/acssensors.7b00305
ACS Sens. 2017, 2, 1302–1309

aligned and ensures a resistance of greater than 100 giga ohms to minimize leakage of current on the actuator electrode into the ISFET.

Modified ISFETs (Figure 5) were assembled into a specialized housing using gold wire bonding to make electrical contact to the

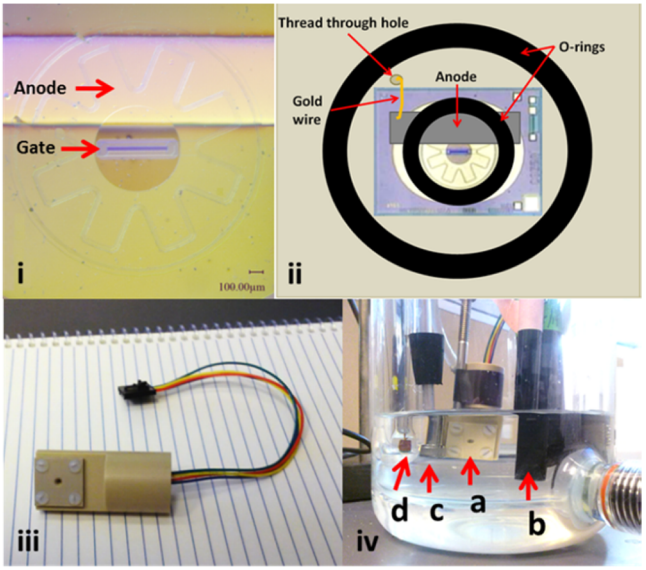

Figure 5. Modified ISFET (i) showing the Pt anode positioned approximately 100 μm from the gate. Electrical contact between the anode is made by threading a gold wire bonded to the topside of the ISFET through two o-rings to the interior of the housing (ii). The fully assembled housing is shown in panel iii. In the bottom right panel (iv) the modified ISFET (a) is positioned in the jacketed beaker with a reference electrode (b), counter electrode (c), and the cathode (d).

source, drain, and substrate on the backside of the ISFET. Encapsulation was achieved by a mechanical means using a series of o-rings. Electrical contact was made to the actuator electrode (anode) on the topside of the ISFET by threading a gold wire bonded to the electrode through the series of o-rings to the inside of the housing. The Nernstian response of the modified ISFETs was assessed in NIST buffers with pH ranging from 4 to 11. The sensor system comprised the modified ISFET with actuator anode, Ag/AgCl reference electrode, titanium counter electrode, and platinum cathode.

The proprietary Honeywell electronics for operating the ISFET required modification to increase the I_{DS} feedback speed and to measure diagnostic variables including leakage currents (I_{L1} and I_{L2}) and drain to source voltage and current (V_{DS} and I_{DS}) as well as the actuating current and corresponding voltage on the anode (I_A and V_A). Simultaneous measurements of V_{RS}, leakage currents, I_A, and V_A, as well as programmable control over I_A served as critical diagnostic and development tools. Standalone electronics and embedded software were developed to provide the groundwork for enabling field deployment and integration with autonomous platforms. A custom ARM microcontroller (TI Cortex TM4C123G) was utilized to provide a programmable actuator with output I_A and V_A monitoring circuitry as well as the modified Honeywell circuitry for operating the ISFET and for monitoring system integrity. Software was developed using Code Composer Studio integrated development environment in C/C++ for basic operation of the pH–A_T sensor.

Analytical Assessment. Initial sensor performance was tested by generating a series of solutions over a range A_T by volumetric dilution (using deionized water with NaCl background) of two solutions of known A_T. The first solution was prepared from $Na_2CO_3(s)$ + $NaHCO_3(s)$ in 0.5 mol kg^{-1} NaCl background. The second solution of known A_T was a natural seawater sample collected at sea, and measured on a conventional benchtop analyzer, standardized using seawater CO_2 Certified Reference Materials.[37] The target mass of the starting solutions was 200 and 130 g for the prepared carbonate solution and seawater sample, respectively. Limited seawater supply necessitated using the bare minimum sample required to submerge all sensor components. Each aliquot of water (prepared with 0.5 mol kg^{-1} NaCl background) for diluting the solution was 5.15 and 2.53 g for the prepared carbonate solution and seawater sample, respectively, and was delivered using a high precision milliGAT pump. We estimate that the initial solutions were known to better than 5 μmol kg^{-1}; and the volumetric additions of H_2O did not significantly alter the accuracy of subsequent dilutions to more than a few μmol kg^{-1}, which is less than the resolution of the sensor.

The operating current for proton generation was set to a constant value ranging from 10 to 40 μA. Standard dilutions were performed by adding 10 aliquots of deionized water with NaCl background to dilute solutions from the starting known A_T down to the lower limit of oceanic A_T (~2100 μmol kg^{-1}). Twenty titration curves were recorded at each sample concentration and a submersible pump was run for 15 s to flush the surface of the ISFET followed by a 5 s hold to allow the solution to settle between titrations. All analyses were performed in a jacketed beaker to maintain sample temperature near ambient at 22.5 °C. The sampling rate was set to 20 Hz for V_{RS} and 2k Hz for diagnostic measurements (I_{L1}, I_{L2}, I_A, V_A, V_{DS}). Signal processing of raw data collected from the ARM board was carried out in Matlab. At each concentration, the titration curves were smoothed and the last 15 end points, corresponding to the final inflection point of the titration, were averaged.

RESULTS

Titration curves produced in standard solutions of HCO_3^- and CO_3^{2-} in 0.5 M NaCl background are shown in Figure 6. The

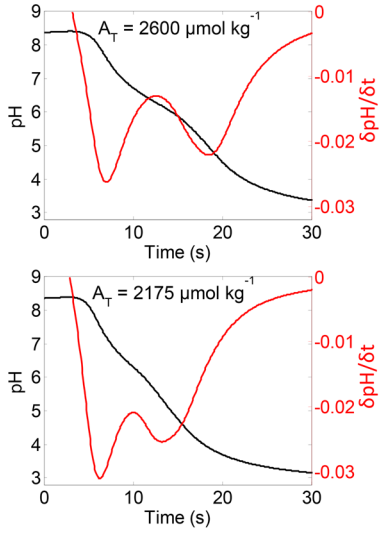

Figure 6. Titration curve (black) and first derivative (red) for standard solutions of HCO_3^- and CO_3^{2-} in 0.5 M NaCl background with A_T of 2600 (top) and 2175 (bottom) μmol kg^{-1}. The first inflection point corresponds to CO_3^{2-} end point and the second inflection point corresponds to the A_T. The time required to reach the A_T end point decreased from ~18 s for the solution with greater A_T to ~13 s for the solution with reduced A_T as anticipated.

first inflection point corresponds to t_{end} for CO_3^{2-} and the final inflection point corresponds to t_{end} for A_T. Standard dilutions of the prepared solution of HCO_3^- and CO_3^{2-} in 0.5 M NaCl background with starting A_T of 2600 μmol kg^{-1} down to ~2100 μmol kg^{-1} are shown in Figure 7. The error analysis in Figure 7 was performed by repeating the measurement 15 times in one solution and the error bars represent standard deviation from the mean at each concentration. Excellent linearity between the A_T and $(t_{end})^{1/2}$ was observed over the range of seawater A_T

DOI: 10.1021/acssensors.7b00305
ACS Sens. 2017, 2, 1302–1309

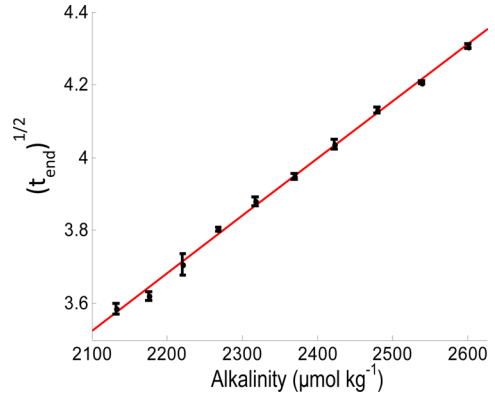

Figure 7. Standard dilution of a prepared solution of HCO_3^- and CO_3^{2-} in 0.5 M NaCl background with a starting A_T of 2600 μmol kg^{-1}. Excellent linearity is observed over the range of seawater A_T (~2200−2500 μmol kg^{-1}) with an R^2 of 0.999 and mean standard deviation of ±7.6 μmol kg^{-1}.

with an R^2 of 0.999, slope of 0.0016, and mean standard deviation of ±7.6 μmol kg^{-1}. Standard dilutions performed repeatedly in seawater with a starting A_T of 2450 μmol kg^{-1} yielded a similar result as shown in Figure 8 with an R^2 of 0.998, slope of 0.0014, and mean standard deviation of ±11 μmol kg^{-1}.

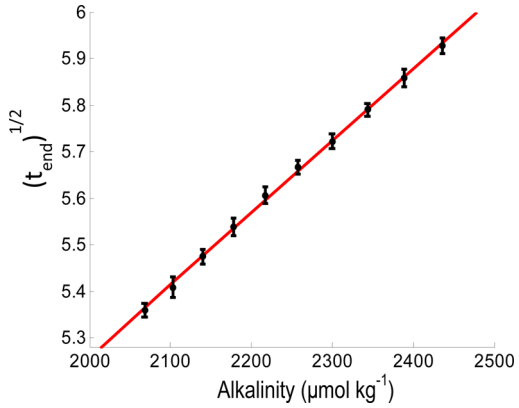

Figure 8. A_T as a function of time ($s^{0.5}$) for the standard dilution of seawater collected in the North Indian Ocean with a starting A_T of 2450 μmol kg^{-1}. Excellent linear relationship is observed over the range of seawater A_T with an R^2 of 0.998 and mean standard deviation of ±11 μmol kg^{-1}.

Distance of the actuator electrode from the ISFET gate as well as current density was not identical between the modified ISFETs used to produce Figures 7 and 8 resulting in slight differences in the slope and the time required to reach t_{end} over the investigated range of A_T. With knowledge of actuator−gate distance, current density, and proton evolution efficiency, the data in Figures 7 and 8 could be used to calculate a mean diffusion coefficient for seawater A_T, which would, in theory, approximate that of the bicarbonate ion (the most abundant component). However, we have not yet developed protocols to evaluate proton evolution efficiency for the actuator, which is not 100% for Pt in the presence of Cl^-, and therefore do not attempt to report diffusion coefficients in this work.

An example of output diagnostic measurements is shown in Figure 9. Optimal values for I_{L1} and I_{L2} are less than 20 and 10 nA, respectively. Values much greater than this are indicative of

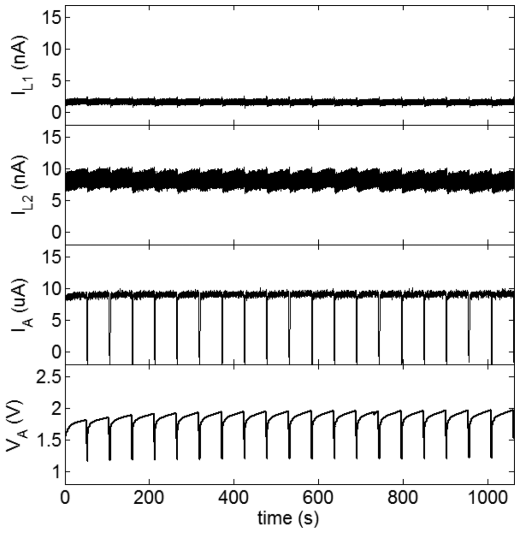

Figure 9. Diagnostic measurements I_{L1} (a), I_{L2} (b), I_A (c), and V_A (d) recorded during 20 titrations in seawater. Each titration was run for approximately 50 s.

inferior ISFET performance and interference of the actuator electrode. I_A and corresponding V_A on the anode were monitored to verify the current was constant and reached the input set point during the titration.

It was determined that an operating current between 10 and 15 μA was required to fully resolve the two end points (see Figure 6) over the range of seawater A_T for sensors with the actuator electrode positioned between 100 and 150 μm from the gate of the ISFET. This corresponds to reaching the end point of the titration in ~25−40 s.

DISCUSSION

Modification of the fully processed ISFET chips was limited to backend processing techniques; typical processing procedures could not be used without damaging the integrity of the fully processed ISFET chip. This resulted in using nonstandard procedures for depositing an electrode onto the surface of the chip. Typically, photolithography would be used to deposit an electrode on the surface of a chip to achieve maximum control over dimension and precise alignment; however, the high temperatures required to deposit a highly insulating SiO_2 film restricted the use of photoresist and necessitated development of a mechanical, nonpolymer, means of patterning the chip. Iterations of shadow mask design and refinement of the alignment of the ISFET in the mask were required to reduce "creep" of deposited material underneath the mask and to more precisely position the electrode within 100−150 μm from the gate.

The actuator electrode could not be deposited directly onto the surface of the ISFET because pathways opened up for current through the chip, detected by disruption in leakage currents. Methods were explored to increase the resistivity between the actuator electrode and the substrate of the chip. Highly insulating SiO_2 is typically thermally deposited at 1000 °C, which is far too high for a fully processed ISFET. Depositing a thick layer of SiO_2 through PECVD became the best option for attaining a highly insulating layer while remaining below the upper limit of temperature exposure for the fully processed ISFET. Other lower temperature methods were tested including argon RF sputtered SiO_2 which allowed

DOI: 10.1021/acssensors.7b00305
ACS Sens. 2017, 2, 1302−1309

use of photolithographic patterning; however, the films were insufficiently insulating.

The voltage required to drive the electrolysis of seawater for generating protons, the proton evolution efficiency, and the stability of proton evolution are a factor of electrode material choice and deposition technique. The proton evolution efficiency need not be 100%, but the short-term stability between titrations is imperative and thus long-term stability of proton evolution will determine the frequency of calibration required. It is anticipated that temperature will have a significant effect on proton generation efficiency over the range of global oceanic temperature (∼−2 to 30 °C). Variable I_A can be applied to achieve optimal proton generation over smaller temperature ranges.

Electrode choice became a critical component of sensor success; it was realized that gold, even though considered ideally inert, could not be used for the electrode material in seawater. Gold was susceptible to dissolution when current was applied in the presence of complexing ions, such as Cl^-, CN^-, and Br^-,[38] and the gold anode visually disappeared in a matter of minutes when current was applied to the anode in seawater or NaCl electrolyte background. Therefore, platinum was used in place of gold as the electrode material for both the anode and cathode. Other electrode materials such as iridium oxide and manganese−molybdenum oxide could be tested to increase proton evolution efficiency in seawater where the oxidation of Cl^- is a competing reaction at the anode during the electrolysis of H_2O.[39,40]

There appears to be a warmup or conditioning of the Pt actuating electrode required to reach a stable measurement. When first powered, running higher current (∼40 μA) for approximately 20 min through the anode was required to achieve stable electrochemical generation of titrant. With short duration pauses (>3 min), there was an upward drift in the time required to reach the end point in the first few titration curves. Therefore, the first 5 measurements were removed in a set of 20 titrations during the standard dilutions. This drift was not observed in continuous measurement mode when the current is turned off for only ∼20 s between titrations, while the pump runs to refresh the surface of the chip.

Additional increases in stability and sensitivity can be achieved by optimizing the sensor, including location of the actuator electrode with respect to the gate, current density, and electrode material. In addition, robust ISFET encapsulation is not trivial and presents a major challenge in terms of both experimental reproducibility and production scalability.[41] Backside contact technology has simplified the use of a mechanical means of encapsulation; however, making electrical connection to the actuator on the topside of the ISFET has required intricate wire bonding techniques to thread the wire between two o-rings to the interior of the housing. This method is not trivial but necessary for utilizing the more robust mechanical seal compared to previous methods of encapsulation that relied on the use of resins. New methods are being explored to integrate the actuator electrode into the sensor housing rather than physically depositing the electrode on the surface of the ISFET. This would remove the direct modification of the ISFET and simplify sensor assembly. Field testing of the current sensor configuration will be achievable after further assessment of sensor calibration and proton generation efficiency over a range of temperature and pressure.

CONCLUSIONS

A microscale, highly insulating coulometric actuator device was integrated with an ISFET, enabling a nanoliter-scale acid−base titration on a single ISFET chip. By placing the actuator electrode on the surface of the ISFET near the gate, the pH can be rapidly measured as the analyte solution is titrated with the electrolytically generated H^+. Here, we applied atypical (back-end processing) techniques to a functional ISFET in order to achieve a sensor-actuator system, demonstrating the CDT technique for the first time using mechanical encapsulation technology and in natural waters, evaluating the method over a very narrow range of oceanic A_T with an eye toward high precision. This sensor is capable of direct, on the fly measurement of the aqueous carbon dioxide system. A single A_T titration can be completed in less than 40 s, no external reagents are required, and there are no complex moving parts making this sensor ideal for autonomous, in situ application. An initial approximate precision of 0.5% A_T was achieved by performing a series of standard dilutions in a prepared solution of HCO_3^- and CO_3^{2-} and in seawater. The estimated resolution of this dual pH−A_T sensor translates to approximately 0.5% and 0.7% error in C_T and pCO_2, respectively, and would enable quantification of biogeochemical processes in rapidly changing environments with strong gradients.

Field applications of the CDT sensor will require thorough calibration over the operational range of temperature, pressure, and salinity in order to account for the effects of, e.g., temperature dependence on proton evolution efficiency and CO_2 hydration/dehydration kinetics. In addition, we have also laid out practical steps such as use of biocides and a closed flow stream that can be used to address the effects of turbulence and biofouling.[24]

AUTHOR INFORMATION

Corresponding Author

*E-mail: trmartz@ucsd.edu.

ORCID

Ellen M. Briggs: 0000-0003-0202-8624
Yuichiro Takeshita: 0000-0003-1824-8517
Andrew C. Kummel: 0000-0001-8301-9855

Present Addresses

[#]Koc University, Physics Department, Istanbul, Turkey
[¶]Monterey Bay Aquarium Research Institute, Moss Landing, California, USA

Author Contributions

The manuscript was written through contributions of all authors. All authors have given approval to the final version of the manuscript.

Notes

The authors declare no competing financial interest.

ACKNOWLEDGMENTS

This work was supported by grant NSF OCE Award 1155122. This material is also based upon work supported by the National Science Foundation Graduate Research Fellowship under Grant No. DGE-1144086. The authors wish to acknowledge Bob Carlson and Jim Connery from Honeywell for kindly providing expert guidance during the development of this sensor. We also thank crew and scientists on GO-SHIP cruise I09N for assisting with collecting seawater for

DOI: 10.1021/acssensors.7b00305
ACS Sens. 2017, 2, 1302−1309

preliminary sensor assessment and two anonymous reviewers for their insightful comments.

REFERENCES

(1) Daly, K. L.; Byrne, R. H.; Dickson, A. G.; Gallager, S. M.; Perry, M. J.; Tivey, M. K. Chemical and Biological Sensors for Time-Series Research: Current Status and New Directions. *Mar. Technol. Soc. J.* **2004**, *38* (2), 121−143.

(2) Prien, R. D. The future of chemical in situ sensors. *Mar. Chem.* **2007**, *107* (3), 422−432.

(3) Johnson, K. S.; Berelson, W.; Boss, E.; Chase, Z.; Claustre, H.; Emerson, S.; Gruber, N.; Körtzinger, A.; Perry, M. J.; Riser, S. Observing Biogeochemical Cycles at Global Scales with Profiling Floats and Gliders: Prospects for a Global Array. *Oceanography* **2009**, *22* (3), 216−225.

(4) Moore, T. S.; Mullaugh, K. M.; Holyoke, R. R.; Madison, A. S.; Yücel, M.; Luther, G. W. Marine Chemical Technology and Sensors for Marine Waters: Potentials and Limits. *Annual review of marine science* **2009**, *1* (1), 91−115.

(5) Martz, T.; Daly, K.; Byrne, R.; Stillman, J.; Turk, D. Technology for Ocean Acidification Research: Needs and Availability. *Oceanography* **2015**, *25* (2), 40−47.

(6) Millero, F. J. The Marine Inorganic Carbon Cycle. *Chem. Rev.* **2007**, *107*, 308−341.

(7) Dickson, A. G.; Riley, J. P. The effect of analytical error on the evaluation of the components of the aquatic carbon-dioxide system. *Mar. Chem.* **1978**, *6* (1), 77−85.

(8) Key, R. M.; Kozyr, A.; Sabine, C. L.; Lee, K.; Wanninkhof, R.; Bullister, J. L.; Feely, R. A.; Millero, F. J.; Mordy, C.; Peng, T. H. A global ocean carbon climatology: Results from Global Data Analysis Project (GLODAP). *Global Biogeochem. Cycles* **2004**, *18* (4), 1.

(9) Carter, B. R.; Toggweiler, J. R.; Key, R. M.; Sarmiento, J. L. Processes determining the marine alkalinity and calcium carbonate saturation state distributions. *Biogeosciences* **2014**, *11* (24), 7349−7362.

(10) Millero, F. J.; Lee, K.; Roche, M. Distribution of alkalinity in the surface waters of the major oceans. *Mar. Chem.* **1998**, *60* (1−2), 111−130.

(11) Lee, K.; Tong, L. T.; Millero, F. J.; Sabine, C. L.; Dickson, A. G.; Goyet, C.; Park, G.-H.; Wanninkhof, R.; Feely, R. A.; Key, R. M. Global relationships of total alkalinity with salinity and temperature in surface waters of the world's oceans. *Geophys. Res. Lett.* **2006**, *33* (19), 1 DOI: 10.1029/2006GL027207.

(12) Bates, N. R.; Michaels, A. F.; Knap, A. H. Alkalinity changes in the Sargasso Sea: geochemical evidence of calcification? *Mar. Chem.* **1996**, *51* (4), 347−358.

(13) Cross, J. N.; Mathis, J. T.; Bates, N. R.; Byrne, R. H. Conservative and non-conservative variations of total alkalinity on the southeastern Bering Sea shelf. *Mar. Chem.* **2013**, *154*, 100−112.

(14) Dickson, A. G.; Afghan, J. D.; Anderson, G. C. Reference materials for oceanic CO2 analysis: a method for the certification of total alkalinity. *Mar. Chem.* **2003**, *80* (2−3), 185−197.

(15) Afshar, M. G.; Crespo, G. A.; Xie, X.; Bakker, E. Direct alkalinity detection with ion-selective chronopotentiometry. *Anal. Chem.* **2014**, *86* (13), 6461−6470.

(16) Li, Q.; Wang, F.; Wang, Z. A.; Yuan, D.; Dai, M.; Chen, J.; Dai, J.; Hoering, K. A. Automated Spectrophotometric Analyzer for Rapid Single-Point Titration of Seawater Total Alkalinity. *Environ. Sci. Technol.* **2013**, *47* (19), 11139−11146.

(17) Martz, T. R.; Dickson, A. G.; DeGrandpre, M. D. Tracer Monitored Titrations: Measurement of Total Alkalinity. *Anal. Chem.* **2006**, *78*, 1817−1826.

(18) Spaulding, R. S.; DeGrandpre, M. D.; Beck, J. C.; Hart, R. D.; Peterson, B.; De Carlo, E. H.; Drupp, P. S.; Hammar, T. R. Autonomous in situ measurements of seawater alkalinity. *Environ. Sci. Technol.* **2014**, *48* (16), 9573−9581.

(19) Afshar, M. G.; Tercier-Waeber, M.; Wehrli, B.; Bakker, E. Direct sensing of total alkalinity profile in a stratified lake. *Geochem. Perspect. Lett.* **2017**, *3* (1), 85−93.

(20) Afshar, M. G.; Crespo, G. A.; Bakker, E. Thin-Layer Chemical Modulations by a Combined Selective Proton Pump and pH Probe for Direct Alkalinity Detection. *Angew. Chem.* **2015**, *127* (28), 8228−8231.

(21) Bergveld, P. Thirty years of ISFETOLOGY: What happened in the past 30 years and what may happen in the next 30 years. *Sens. Actuators, B* **2003**, *88* (1), 1−20.

(22) Martz, T. R.; Connery, J. G.; Johnson, K. S. Testing the Honeywell Durafet for seawater pH applications. *Limnol. Oceanogr.: Methods* **2010**, *8*, 172−184.

(23) Sandifer, J. R.; Voycheck, J. J. A review of biosensor and industrial applications of pH-ISFETs and an evaluation of Honeywell's "DuraFET. *Microchim. Acta* **1999**, *131* (1−2), 91−98.

(24) Bresnahan, P. J.; Martz, T. R.; Takeshita, Y.; Johnson, K. S.; LaShomb, M. Best practices for autonomous measurement of seawater pH with the Honeywell Durafet. *Methods Oceanogr.* **2014**, *9* (0), 44−60.

(25) Johnson, K. S.; Jannasch, H. W.; Coletti, L. J.; Elrod, V. A.; Martz, T. R.; Takeshita, Y.; Carlson, R. J.; Connery, J. G. Deep-Sea DuraFET: A Pressure Tolerant pH Sensor Designed for Global Sensor Networks. *Anal. Chem.* **2016**, *88* (6), 3249−3256.

(26) Baxter, R.; Connery, J.; Fogel, J.; Silverthorne, S. ESD Protection of ISFET sensors; US Patent No 5,407,854, April 18, 1995.

(27) Connery, J. G.; Shaffer, W. Instrument for potentiometric electrochemical measurements; US Patent No 4,851,104, July 25, 1989.

(28) Takeshita, Y.; Martz, T. R.; Johnson, K. S.; Dickson, A. G. Characterization of an Ion Sensitive Field Effect Transistor and Chloride Ion Selective Electrodes for pH Measurements in Seawater. *Anal. Chem.* **2014**, *86* (22), 11189−11195.

(29) Olthuis, W.; Bergveld, P. Integrated coulometric sensor-actuator devices. *Microchim. Acta* **1995**, *121* (1−4), 191−223.

(30) Olthuis, W.; Luo, J.; van der Schoot, B. H.; Bomer, J. G.; Bergveld, P. Dynamic behaviour of ISFET-based sensor-actuator systems. *Sens. Actuators, B* **1990**, *1* (1−6), 416−420.

(31) Olthuis, W.; Van Der Schoot, B. H.; Chavez, F.; Bergveld, P. A dipstick sensor for coulometric acid-base titrations. *Sens. Actuators* **1989**, *17* (1−2), 279−283.

(32) Van der Schoot, B.; Bergveld, P. An ISFET-based microlitre titrator: integration of a chemical sensor—actuator system. *Sens. Actuators* **1985**, *8* (1), 11−22.

(33) Olthuis, W.; Luo, J.; Van der Schoot, B. H.; Bergveld, P.; Bos, M.; Van der Linden, W. E. Modelling of non-steady-state concentration profiles at ISFET-based coulometric sensor—actuator systems. *Anal. Chim. Acta* **1990**, *229* (0), 71−81.

(34) Van der Schoot, B.; Van der Wal, P.; de Rooij, N.; West, S. Titration-on-a-chip, chemical sensor−actuator systems from idea to commercial product. *Sens. Actuators, B* **2005**, *105* (1), 88−95.

(35) Gemene, K. L.; Bakker, E. Direct Sensing of Total Acidity by Chronopotentiometric Flash Titrations at Polymer Membrane Ion-Selective Electrodes. *Anal. Chem.* **2008**, *80* (10), 3743−3750.

(36) Martz, T. Personal Communication with Orion.

(37) Dickson, A. G. Reference material for oceanic CO_2 measurements. *Oceanography* **2001**, *14* (4), 21−22.

(38) Cherevko, S.; Topalov, A. A.; Zeradjanin, A. R.; Katsounaros, I.; Mayrhofer, K. J. J. Gold dissolution: towards understanding of noble metal corrosion. *RSC Adv.* **2013**, *3* (37), 16516−16527.

(39) Venkatkarthick, R.; Elamathi, S.; Sangeetha, D.; Balaji, R.; Suresh Kannan, B.; Vasudevan, S.; Jonas Davidson, D.; Sozhan, G.; Ravichandran, S. Studies on polymer modified metal oxide anode for oxygen evolution reaction in saline water. *J. Electroanal. Chem.* **2013**, *697*, 1−4.

(40) Fujimura, K.; Matsui, T.; Habazaki, H.; Kawashima, A.; Kumagai, N.; Hashimoto, K. The durability of manganese−molybdenum oxide anodes for oxygen evolution in seawater electrolysis. *Electrochim. Acta* **2000**, *45* (14), 2297−2303.

(41) Oelßner, W.; Zosel, J.; Guth, U.; Pechstein, T.; Babel, W.; Connery, J. G.; Demuth, C.; Grote Gansey, M.; Verburg, J. B.

DOI: 10.1021/acssensors.7b00305
ACS Sens. 2017, 2, 1302−1309

Encapsulation of ISFET sensor chips. *Sens. Actuators, B* **2005**, *105* (1), 104−117.

DOI: 10.1021/acssensors.7b00305
ACS Sens. 2017, 2, 1302−1309